Available online at www.sciencedirect.com

SCIENCE DIRECT

Developmental Biology 285 (2005) 238–251

DEVELOPMENTAL BIOLOGY

www.elsevier.com/locate/ydbio

LrrA, a novel leucine-rich repeat protein involved in cytoskeleton remodeling, is required for multicellular morphogenesis in *Dictyostelium discoideum*

Chia-I Liu[a], Tsung-Lin Cheng[b], Shu-Zhen Chen[a], Ying-Chieh Huang[a], Wen-Tsan Chang[a,b,*]

[a]*Department of Biochemistry, National Cheng Kung University Medical College, Tainan 701, Taiwan, ROC*
[b]*Institute of Basic Medical Sciences, National Cheng Kung University Medical College, Tainan 701, Taiwan, ROC*

Received for publication 19 November 2004, revised 7 May 2005, accepted 25 May 2005
Available online 27 July 2005

Abstract

Cell sorting by differential cell adhesion and movement is a fundamental process in multicellular morphogenesis. We have identified a *Dictyostelium discoideum* gene encoding a novel protein, LrrA, which composes almost entirely leucine-rich repeats (LRRs) including a putative leucine zipper motif. Transcription of *lrrA* appeared to be developmentally regulated with robust expression during vegetative growth and early development. *lrrA* null cells generated by homologous recombination aggregated to form loose mounds, but subsequent morphogenesis was blocked without formation of the apical tip. The cells adhered poorly to a substratum and did not form tight cell–cell agglomerates in suspension; in addition, they were unable to polarize and exhibit chemotactic movement in the submerged aggregation and Dunn chamber chemotaxis assays. Fluorescence-conjugated phalloidin staining revealed that both vegetative and aggregation competent *lrrA*$^-$ cells contained numerous F-actin-enriched microspikes around the periphery of cells. Quantitative analysis of the fluorescence-stained F-actin showed that *lrrA*$^-$ cells exhibited a dramatically increase in F-actin as compared to the wild-type cells. When developed together with wild-type cells, *lrrA*$^-$ cells were unable to move to the apical tip and sorted preferentially to the rear and lower cup regions. These results indicate that LrrA involves in cytoskeleton remodeling, which is needed for normal chemotactic aggregation and efficient cell sorting during multicellular morphogenesis, particularly in the formation of apical tip.

Keywords: Leucine-rich repeats (LRRs); Gene knockout; Cell adhesion; Cytoskeleton remodeling; Multicellular morphogenesis; *Dictyostelium discoideum*

Introduction

Leucine-rich repeats (LRRs) are short consensus sequence motifs present in many proteins with diverse functions and subcellular localizations. They appear to be generally involved in protein–protein interactions (Kobe and Deisenhofer, 1994, 1995). LRRs motif-containing proteins not only participate in many biologically important processes, such as signal transduction, cell adhesion, disease resistance and innate immune response (Buchanan and Gay, 1996), but also involve in cell polarization (Bilder and Perrimon, 2000), apoptosis signaling (Inohara and Nunez, 2001, Inohara et al., 1999), mammalian development (Tong et al., 2000a,b) and cytoskeleton remodeling (Xu et al., 1997; Wu et al., 2000).

LRRs are usually present in tandem with the number of repeats among 1–30 (Buchanan and Gay, 1996). The most common length of a LRR is 24 residues, but repeats containing between 20 and 29 residues have been described (Buchanan and Gay, 1996). There is a distinctive subgroup of LRRs that are 23 amino acids in length instead of 24 and which contain additional consensus residues, especially proline (Fig. 1). These proteins have in common an ability to associate with the Ras family of signaling GTPases (Buchanan and Gay, 1996), such as the middle-repetitive repeat region in *Saccharomyces cerevisiae* adenylyl cyclase

* Corresponding author. Department of Biochemistry, National Cheng Kung University Medical College, Tainan 701, Taiwan, ROC. Fax: +886 6 2741694.
E-mail address: wtchang@mail.ncku.edu.tw (W.-T. Chang).

0012-1606/$ - see front matter © 2005 Elsevier Inc. All rights reserved.
doi:10.1016/j.ydbio.2005.05.045

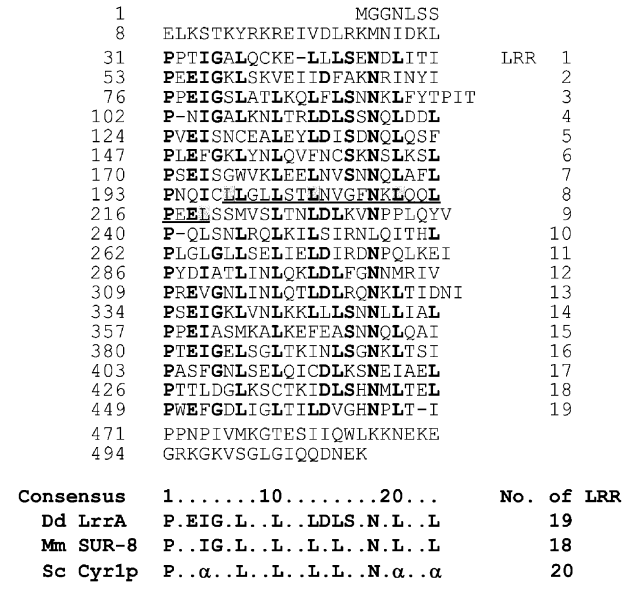

Fig. 1. Amino acid sequence and LRR motif structure of the LrrA protein. The full-length amino acid sequence of LrrA protein was predicted from its cDNA sequence. Leucine zipper motif (amino acids 198–219) is underlined, and consensus leucines are shaded. The nineteen LRR motifs (amino acids 31–470) are aligned, and the numbers of the motifs are indicated. Consensus amino acids are indicated in bold and shown below with the consensus of Dd LrrA (AF200466), Mm SUR-8 (AF068921), and Sc Cyr1p (M12057) LRRs. α, aliphatic residue (A, V, L, I, F, Y, or M).

(Cyr1p) mediates interaction of the cyclase with RAS proteins (Field et al., 1990; Suzuki et al., 1990), and the LRR protein SUR-8 in *Caenorhabditis elegans* and mammals acts as a scaffold and forms a complex with Ras and Raf (Sieburth et al., 1998; Li et al., 2000).

The cellular slime mould *Dictyostelium discoideum* grows as a unicellular amoeba but undergoes a relatively simple multicellular development. During early aggregation stage, amoebae move chemotactically towards cAMP, make contact and join into streams that in turn collect into hemispherical mounds of up to 10^5 cells (Devreotes, 1989; Firtel, 1995; Chen et al., 1996; Parent and Devreotes, 1996). Within each multicellular assembly, amoebae differentiate autonomously and randomly into prespore and prestalk cells (Early et al., 1995; Firtel, 1995, 1996; Shaulsky and Loomis, 1996). The prestalk cells then move differentially to the apex of the mound, where they form a tip that acts as an organizing center (Rubin and Robertson, 1975; Williams et al., 1989; Clow and McNally, 1999; Kellerman and McNally, 1999; Nicol et al., 1999; Clow et al., 2000; Firtel and Meili, 2000). This tip elongates and falls over to form a migrating slug, or pseudoplasmodium, within which prestalk and prespore cells organize along an anterior–posterior axis pattern. In response to environmental signals, the slug undergoes culmination, resulting in the formation of a mature fruiting body containing terminally differentiated spores and stalk cells (Gross, 1994; Parent and Devreotes, 1996; Aubry and Firtel, 1999).

During tip formation and subsequent morphogenesis, cell sorting is mediated by differential chemotaxis to cAMP via similar chemotaxis pathways and differential cell adhesion systems (Traynor et al., 1992; Reymond et al., 1995; Firtel and Meili, 2000; Dormann et al., 2000; Verkerke-van Wijk et al., 2001). Therefore, interfering with cAMP signaling by disrupting a prestalk cell specific cAMP receptor subtype 2 (CAR2) (Saxe et al., 1993), overproducing the secreted form of cAMP phosphodiesterase (Traynor et al., 1992) or disrupting genes encoding components involved in cytoskeleton remodeling, such as F-actin cross-linking proteins (Witke et al., 1992), myosin heavy chain (Traynor et al., 1994), myosin II regulatory light chain (Clow et al., 2000) and *limB* (Chien et al., 2000), block development at the mound stage. Similarly, disrupting genes encoding components involved in either cell-type determination or differential cell sorting, such as tipA (Stege et al., 1997), as well as involved in cell–cell adhesion, such as *lagC* (Dynes et al., 1994; Wang et al., 2000; Kibler et al., 2003) and *dtfA* (Ginger et al., 1998), arrests development prior to formation of the apical tip.

To identify novel genes involved in pattern formation of multicellular development in *D. discoideum*, we searched genomic and cDNA databases (All Dictyostelium BLAST Search [http://www.dicty.sdsc.edu/]) for homologues of *S. cerevisiae* Cyr1p, whose LRRs motif is essential for interaction with Ras proteins (Field et al., 1990; Suzuki et al., 1990). We identified a novel protein constituted entirely of tandem repeats of the LRRs motif. Analysis of an *lrrA* null mutant indicates that LrrA plays a decisive role in multicellular morphogenesis, especially in apical tip formation.

Materials and methods

Cell and molecular biology methods

Cell culture, development and transformation of *D. discoideum* cells, Southern, Northern and Western blotting and *lacZ* reporter analysis have all been described previously (Chang et al., 1995, 1996; Huang et al., 2004). Molecular cloning and analysis approaches are standard as described by Sambrook et al. (1989) and Ausubel et al. (1998).

Cellular location of LrrA protein

The complete *lrrA* coding sequence (encoding amino acids 1–510) and a mutant version with the leucine zipper motif deleted (deleting amino acids 197–321) were created by PCR from the full-length *lrrA* cDNA with the appropriate primers and were cloned into the pAct15-GFP plasmid. The resulting constructs contained the wild-type or mutated *lrrA* coding sequence fused in-frame with the DNA sequence for the green fluorescent protein (GFP-C3) (Crameri et al., 1996) under the control of the actin 15 promoter and actin 8 terminator. These constructs were used for transformation of

wild-type Ax2 and *lrrA*$^-$ cells by electroporation, selecting for resistance to G418.

Generation of lrrA null mutants

To effectively target the *lrrA* locus in the *D. discoideum* genome, we created two *lrrA* knockout constructs, *Bgl*II-KO and *Sna*BI-KO (see Supplementary data, Supplementary Fig. 1A) as described previously (De Lozanne, 1987). Constructs were made containing 1.2 kb (*Bgl*II-KO) and 1.6 kb (*Sna*BI-KO) of *lrrA* genomic DNA with a blasticidin S-resistance cassette (Bsr^r) inserted into the coding sequence in the same orientation in each construct, so that its strong actin 8 termination sequence blocked any transcriptional read through. Transformants were then plated on SM-agar with *K. aerogenes* as a food source and developed. Colonies that displayed aberrant developmental morphology were picked from the SM-agar plates and recloned. The insertional mutants obtained were analyzed by Southern and Northern blotting to verify disruption of the *lrrA* gene.

Complementation by transformation

The complete *lrrA* coding sequence (encoding amino acids 1–510) was generated by PCR from the full-length *lrrA* cDNA with the appropriate primers and cloned into the pAct15-GST plasmid (Huang et al., 2004). The resulting construct contained the wild-type *lrrA* cDNA fused in-frame with DNA for glutathione *S*-transferase (GST) under the control of the actin 15 promoter and actin 8 terminator. The constructs, act15-lrrA-gst and act15-gst, were used for complementation of *lrrA* null mutant *Sna*BI-KO using electroporation and selection for resistance to G418.

Cell-substratum adhesion assay

The cell-substratum adhesion assay was adopted from Vogel (1987) and Chen and Katz (2000). Exponentially grown cells were harvested and washed three times with Sorensen buffer and resuspended to 1×10^6 cells/ml in the same buffer. Four milliliter of this suspension was incubated in 50 ml glass cell culture flasks on a gyratory shaker at 120 rpm for 10 min at room temperature. The cells were incubated for a further 40 min without shaking to allow them to adhere. After that, the flasks were agitated gently for 3 min at 60 rpm, and the supernatants were transferred to a test tube. Non-adherent cells in each supernatant were determined using a hemacytometer.

Cell agglutination assay

The cell agglutination assay was performed as described by Varney et al. (2002). Exponentially grown cells were harvested and washed three times with KK_2 buffer and resuspended to 3×10^6 cells/ml in the same buffer. Two milliliter of the suspension was transferred to a plastic Falcon 2059 15-ml test tube (BD Biosciences, San Jose, CA) and left for 6 h at 22°C on a rotary wheel set to 45 rpm. Samples were then removed from the tubes with a Pasteur pipette and overlaid onto a borosilicate cover slip for photography.

F-actin staining by Alexa Fluor 488-conjugated phalloidin

For F-actin staining, vegetative cells from axenic culture or agglutination-competent cells were deposited onto glass cover slips for 10 min, fixed in 3.7% formaldehyde solution for 10 min, permeabilized in 0.2% Triton X-100 solution for 5 min and stained with Alexa Fluor 488-conjugated phalloidin solution (Molecular Probes, Eugene, OR) for 20 min. The amount of F-actin was analyzed by flow cytometry. The flow cytometry measurements were performed at a FACS-Calibur™ flow cytometer (BD Biosciences, San Jose, CA).

Dunn chamber chemotaxis assay

The chemotactic migration assay of *D. discoideum* cells was assessed by directly observation and recording of cell behavior in stable concentration gradients of chemoattractant, cAMP or folic acid, using the Dunn chemotaxis chamber (Weber Scientific International Ltd., Teddington, UK) (Zicha et al., 1991; Webb et al., 1996; Allen et al., 1998). Chemoattractants added to the outer well of the apparatus diffuse across the annular bridge to the inner blind well of the chamber and form a gradient. In these experiments, the outer well of the chamber was filled with developing buffer containing 10 μM of cAMP or 100 μM of folic acid and the concentric inner well with only developing buffer. Cover slips with cells were inverted onto the Dunn chamber, and cell migration was observed through the annular bridge between the concentric inner and outer wells.

Aggregation in submerged monolayers

Exponentially grown cells were harvested and washed three times with aggregation buffer (pH 6.2). Four milliliter of the cell suspension was plated in 5-cm tissue culture dishes (Nalge Nunc International, Rochester, NY) to a final density of 2×10^5 cells/cm^2. Cells were incubated at 22°C in a humid box.

Accession number

The DDBJ/EMBL/GenBank accession number for the *lrrA* gene is AF200466 and for the *lrrA* promoter is AF388909.

Results

Identification of the leucine-rich repeat protein LrrA

By searching the expressed sequence tag (EST) database of Dicty_cDB (http://www.csm.biol.tsukuba.ac.jp/cDNA/

database.html) with the *S. cerevisiae* adenylyl cyclase (Cyr1p) amino acid sequence (Kataoka et al., 1985), we identified a cDNA clone FCL-AC05, which has homology to the Cyr1p LRR motif. The cDNA contains one long open reading frame of 1530 bp that encodes a predicted protein of 510 amino acids with a calculated molecular mass of 57 kDa. It contains 19 tandem repeats of the LRR motif (amino acids 31–470), including a putative leucine zipper motif (amino acids 198–219) (Fig. 1). The full-length cDNA includes 284 bp of 5′-untranslated sequence and 71 bp of 3′-untranslated sequence. Sequencing the genomic DNA revealed a single intron interrupting the coding sequence of *lrrA* (data not shown).

Alignment of the high scoring segments obtained from a BLAST search of the non-redundant NCBI database (http://www.ncbi.nlm.nih.gov/BLAST/) using the deduced amino acid sequence of the isolated cDNA coding region revealed that the putative product displayed weak similarity to SUR-8, which is a positive regulator of Ras signaling that enhances MAP kinase activation and forms a complex with Ras and Raf (Sieburth et al., 1998; Li et al., 2000). Since the predicted protein was composed almost entirely of LRR motifs, the gene was designated as *lrrA*. Searching the non-redundant NCBI database, as well as the *D. discoideum* genomic and cDNA databases (All Dictyostelium BLAST Search; http://dicty.sdsc.edu/) with the *lrrA* nucleotide sequence failed to reveal any other related genomic matches, indicating that *lrrA* is a unique gene.

Analysis of the lrrA gene

The temporal expression pattern of *lrrA* during development was determined by extracting RNA at various times of development and hybridizing with full-length *lrrA* cDNA. *lrrA* encodes a single transcript of 1.6 kb that is substantially expressed during vegetative growth. We observed that *lrrA* expression increased upon starvation, peaked at 6–9 h of the aggregation stage and declined abruptly from 16 h of development (Fig. 2A).

To identify the spatial pattern of *lrrA* expression during development, we isolated and sequenced the *lrrA* promoter region including the partial coding sequence of the upstream *clcA* gene (AF414428) and made a reporter construct with the *Escherichia coli lacZ* gene under its control. A strain harboring this construct was developed on KK_2 buffered-agar, fixed and stained with X-gal. All cells stained strongly during early development. However, the pattern of expression in first fingers and early culminates became progressively decreased in the staining cells. In fruiting bodies, both the spore and stalk cells exhibited weak staining with X-gal (data not shown).

Amino acid sequence analysis indicated that LrrA did not contain any putative targeting sequences or transmembrane domains, suggesting that LrrA is a cytoplasmic protein. To localize LrrA within the cell, constructs driven

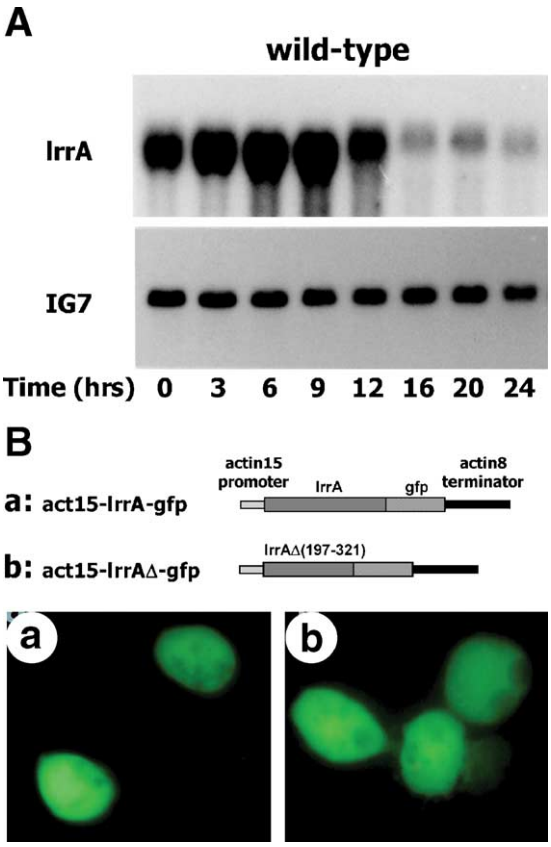

Fig. 2. Developmental expression of the *lrrA* gene and subcellular localization of the LrrA protein. (A) Northern blot analysis of the *lrrA* gene expression. RNAs extracted at various times during development was probed with the full-length *lrrA* cDNA, and with IG7, a gene that is expressed at a constant level during development. Amoebae aggregated by 6 h, formed mounds by 9 h, formed tipped aggregates by 12 h, slugs by 16 h, reached late culmination by 20 h and formed mature fruiting bodies by 24 h. (B) Fluorescence images of the GFP-C3 fusion constructs of the complete *lrrA* coding sequence (encoding amino acids 1–510) (a) or mutant with deleted leucine zipper motif (deleting amino acids 197–321) (b), fused in-frame with DNA for the green fluorescent protein (GFP-C3) under the control of the actin 15 promoter and actin 8 terminator.

by the actin 15 promoter were made with either full-length *lrrA* or using a mutant with deleted leucine zipper motif fused in-frame with the highly sensitive C3 version of the green fluorescent protein (GFP) (Crameri et al., 1996). Localization of the GFP fusion protein in both the *act15-lrrA-gfp* and *act15-lrrAΔ-gfp* transformants was uniform throughout the cells at all times during development (Fig. 2B). These results were consistent with LrrA being a cytosolic protein.

Disruption of the lrrA gene

To investigate the function of LrrA protein during *D. discoideum* growth and development, two independent *lrrA* knockout strains were generated specifically (see Materials and methods). Disruption of the *lrrA* gene was confirmed by Southern blot (see Supplementary data, Supplementary Fig. 1B) and Northern blot analyses using

an upstream *lrrA* DNA fragment as a probe. No transcripts were found in both the *Bgl*II-KO and *Sna*BI-KO mutants (data not shown). Efficiency of the homologous recombination with both the *Bgl*II-KO and *Sna*BI-KO targeting constructs was approximately 30%. All of the isolated mutants displayed identical phenotypes. The *lrrA*$^-$ cells grew normally in association with *K. aerogenes* on SM-agar plate and in liquid axenic medium (data not shown). During development, the cells aggregated and formed mounds with the similar timing as that of the wild-type cells, but the mounds failed to form apical tips both on bacterial lawns (data not shown) and on KK_2 agar (Fig. 3). However, the loose mounds formed by *lrrA*$^-$ cells were significantly larger than those formed by the wild-type cells (Fig. 7A).

To confirm that the phenotype was caused by disruption of *lrrA*, we transformed *lrrA*$^-$ cells with an *lrrA* expression construct fused in-frame with the glutathione *S*-transferase (GST), under the control of the actin 15 promoter. The results revealed that only the expressed LrrA-GST fusion construct restored the ability of *lrrA* null cells to develop normally and produce mature fruiting bodies of essentially wild-type appearance (Fig. 3), consistent with a fully functional LrrA-GST fusion. Expression of the LrrA-GST fusion protein was verified by Western blot analysis using anti-GST antibody (see Supplementary data, Supplementary Fig. 2).

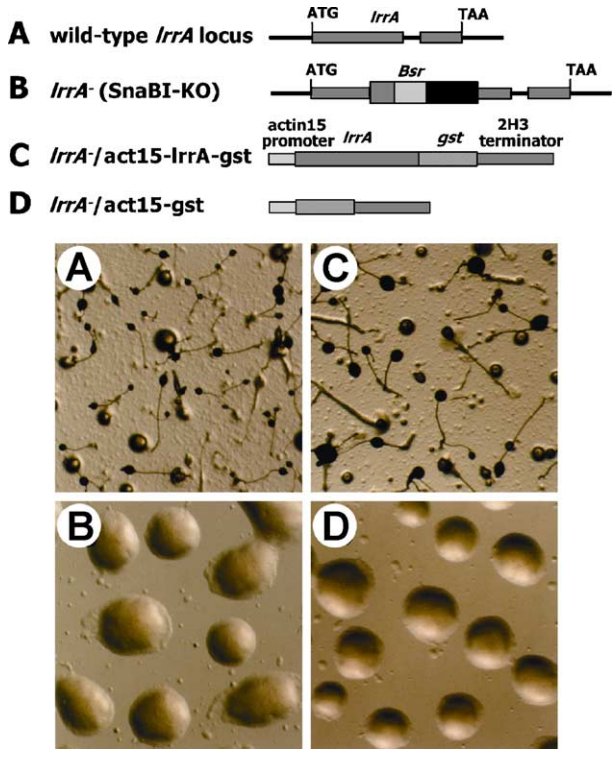

Fig. 3. Phenotype and complementation of the *lrrA* null mutation. Terminal structures formed by wild-type *lrrA* locus (A), *lrrA*$^-$ mutant *Sna*BI-KO strain (B), *lrrA*$^-$/act15-lrrA-gst transformant (C), and *lrrA*$^-$/act15-gst transformant (D) on KK_2 agars, photographed after 24 h of development.

Effects on cell adhesion and cytoskeletal F-actin

The earliest detectable phenotypic trait in the mutant cells was their weak adhesion to the surfaces of plastic petri dishes, as revealed by their detachment upon gentle pipetting or even suspension in the axenic medium without any attachment to the surface (data not shown). To investigate this phenotypic trait directly, we measured their adhesion to the substratum and to other cells. The cell substratum adhesion assay quantifies the ability of amoebae to attach to a glass surface (Vogel, 1987; Chen and Katz, 2000). Wild-type and *lrrA*$^-$ cells were allowed to attach to the bottom of glass cell culture flasks prior to gentle and brief agitation. The non-adherent cells were then counted. Wild-type cells adhered more than did the *lrrA*$^-$ cells (Fig. 4A).

Microscopic examination of vegetative cells growing in plastic petri dishes for 24 h revealed that wild-type cells displayed an elongated and polarized appearance, while *lrrA*$^-$ cells exhibited a rounded and nonpolar morphology (Fig. 4B). To examine this difference directly, we stained the actin cytoskeleton in wild-type and *lrrA*$^-$ cells from axenic culture with Alexa Fluor 488-conjugated phalloidin. In wild-type cells, the majority of F-actin was recruited into the macropinocytic crowns, whereas in *lrrA*$^-$ cells, the F-actin was enriched in cell surface projections as microspikes (Fig. 4C). To determine more precisely the levels of F-actin, the amount of fluorescence-stained F-actin was analyzed using a fluorescence-activated cell sorter. The levels of F-actin in the *lrrA*$^-$ cells were markedly elevated with respect to the wild-type cells (Fig. 4D). These results indicated that vegetative *lrrA*$^-$ amoebae were defective in organization of the actin cytoskeleton.

When *D. discoideum* cells were washed free of growth medium, resuspended in non-nutrient buffer and shaken in suspension, large cell agglomerates formed (Varney et al., 2002). The agglomerates formed by *lrrA*$^-$ cells starved in KK_2 buffer for 6 h were significantly smaller and looser than those formed by wild-type cells (Fig. 4E). Microscopic examination of the *lrrA*$^-$ cells showed that they were rounded and had many microspikes around their periphery and appeared not to be polarized, suggesting an aberrant organization of the actin cytoskeleton. To examine this idea directly, we stained the actin cytoskeleton in wild-type and *lrrA*$^-$ cells with Alexa Fluor 488-conjugated phalloidin. F-actin was observed to be highly localized to the anterior leading edge and to a lesser degree in the posterior region of polarized agglutination-competent wild-type cells (Fig. 4F). In contrast, *lrrA*$^-$ cells possessed many F-actin-enriched microspikes around the periphery of the cells (Fig. 4F). To determine more precisely the levels of F-actin, the amount of fluorescence-stained F-actin was analyzed using a fluorescence-activated cell sorter. The levels of F-actin in the *lrrA*$^-$ cells were dramatically elevated with respect to the wild-type cells (Fig. 4G), indicating that aggregation competent *lrrA*$^-$ cells were markedly defective in the regulation of F-actin organization.

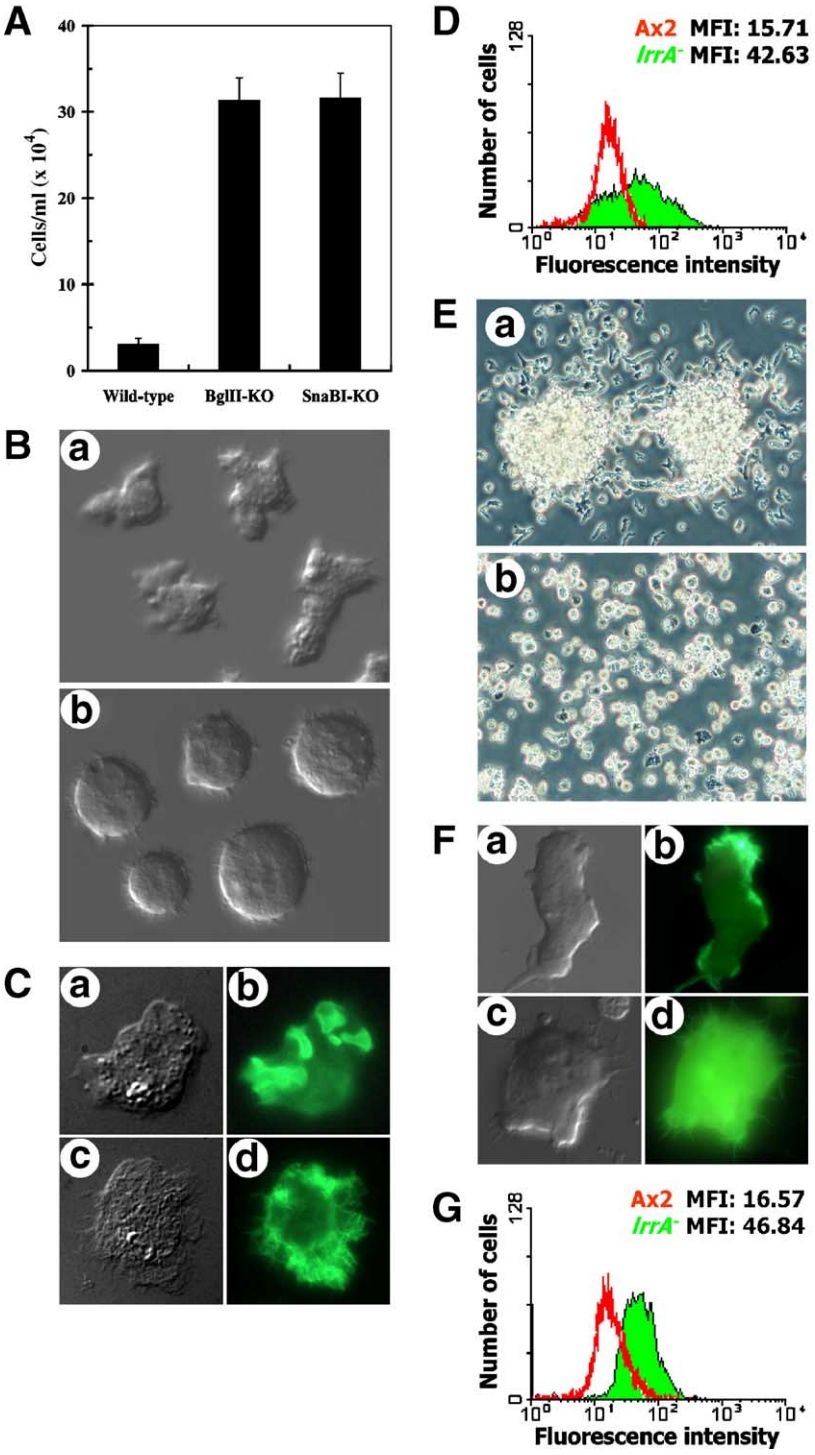

Fig. 4. Effect of the *lrrA* null mutation on cell adhesion and actin cytoskeleton. (A) Cell-substratum adhesion assay. The numbers of non-adherent cells were counted in the supernatants from glass cell culture flasks in a hemacytometer. (B) DIC images of wild-type Ax2 (a) and *lrrA*$^-$ (b) cells growing in plastic petri dishes for 24 h. (C) F-actin distribution in wild-type Ax2 (a and b) and *lrrA*$^-$ (c and d) cells during vegetative growth. Exponentially growing cells were cultured on a glass surface for 24 h before fixation and staining with Alexa Fluor 488-conjugated phalloidin as described in Materials and methods. (D) Histogram plots of the levels of fluorescence-stained F-actin in wild-type Ax2 (red) and *lrrA*$^-$ (green) cells growing in axenic medium for 24 h. (E) Representative photographs of cell agglomerates and morphologies that formed after 6 h of starvation in the cell agglutination assay are shown: a, wild-type Ax2 cells; b, *lrrA*$^-$ cells. (F) Visualization of filopodia on wild-type Ax2 (a and b) and *lrrA*$^-$ (c and d) cells at the aggregation stage. F-actin was stained with Alexa Fluor 488-conjugated phalloidin after fixation of aggregation-competent cells on a glass surface. (G) Histogram plots of the levels of fluorescence-stained F-actin in wild-type Ax2 (red) and *lrrA*$^-$ (green) cells at the aggregation stage. MFI represents the mean fluorescence intensity.

Effects on chemotactic response

It is known that cAMP is especially active as a chemotactic agent during the aggregation stage and shows relatively little activity during the vegetative growth. To analyze the effect of *lrrA* mutation on chemotactic migration at the aggregation stage, we examined the chemotactic responsiveness of wild-type and *lrrA*$^-$ cells to gradients of cAMP after 6 h of starvation in shaken suspension without or with addition of 100 nM cAMP pulses every 6 min. The chemotactic responsiveness to cAMP was observed in wild-type aggregating cells, whereas *lrrA*$^-$ cells were totally unresponsive to gradients of cAMP (Fig. 5A). Similar results were also observed when chemotaxis assays were conducted on aggregating cells that had been pulsated with 100 nM cAMP for 6 h (Fig. 5B). This defect in chemotactic migration is consistent with the observed F-actin distribution and cellular morphology of *lrrA*$^-$ cells.

In *D. discoideum* cells, reorganization of the actin cytoskeleton is essential for cellular motility in response to chemotactic agents. During vegetative growth, amoebae are chemotactic to folic acid, which is specifically secreted by bacteria and is used in food seeking (Pan et al., 1972, 1975).

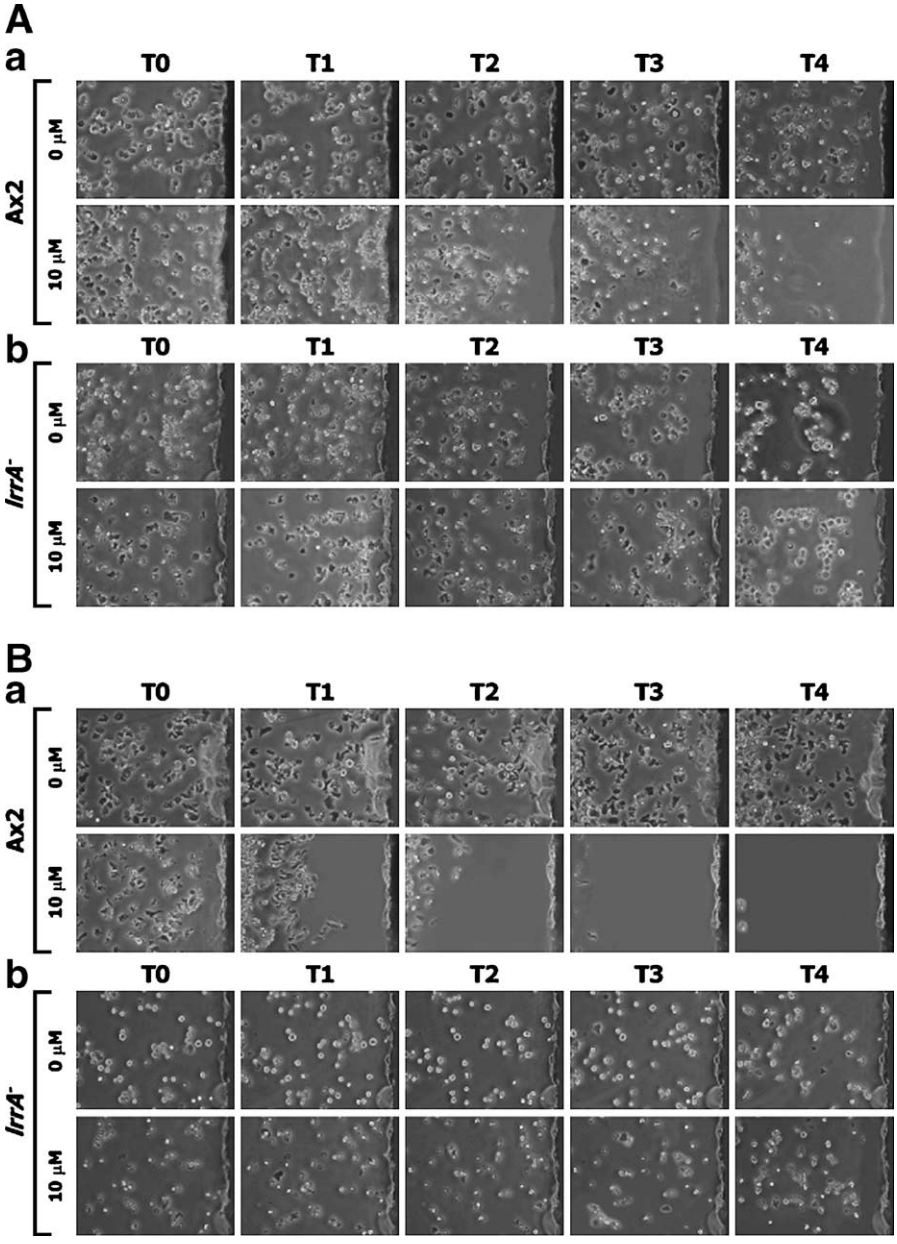

Fig. 5. Dunn chamber chemotaxis assay of the *lrrA*$^-$ cells to gradients of cAMP. Wild-type Ax2 and *lrrA*$^-$ cells were developed for 6 h in shaken suspension without (A) or with (B) addition of 100 nM cAMP pulses every 6 min then washed once in developing buffer just before plating. The cells were plated on cover slips, and then the cover slips with cells were inverted onto the Dunn chamber slide. Developing buffer in outer well contained 10 μM of cAMP as indicated. The photographs were taken every hour after setting up the Dunn chamber. The inner well is toward the right.

To assess the effect of *lrrA* mutation on cellular motility at the vegetative phase, we examined the chemotactic responsiveness of wild-type and *lrrA*$^-$ cells from axenic culture and starved for 6 h in shaken suspension to gradients of folic acid. Wild-type vegetative amoebae exhibited strongly chemotactic responses to gradients of folic acid at concentration 100 μM, whereas *lrrA*$^-$ cells were totally unresponsive to gradients of folic acid (Fig. 6A). Similar results were also observed when chemotaxis assays were conducted on cells that had been starved for 6 h in shaken suspension (Fig. 6B). The results were consistent with the chemotactic properties to gradients of cAMP observed during aggregation stage.

Effects on multicellular morphogenesis

To analyze in detail the effect of *lrrA* null mutation on multicellular development, we characterized several aspects of the development of *lrrA*$^-$ cells. Firstly, we examined aggregation of the cells at different cell densities on KK_2 agar. The *lrrA*$^-$ cells aggregated efficiently even at very low densities, whereas wild-type cells were delayed in their aggregation and produced larger loose mounds. The mutant cells never formed streams at any cell density (Fig. 7A). In addition, in the submerged monolayer aggregation assay, *lrrA*$^-$ cells did not polarize properly and exhibited severe impairment in chemotaxis (Fig. 7B). In contrast, the wild-

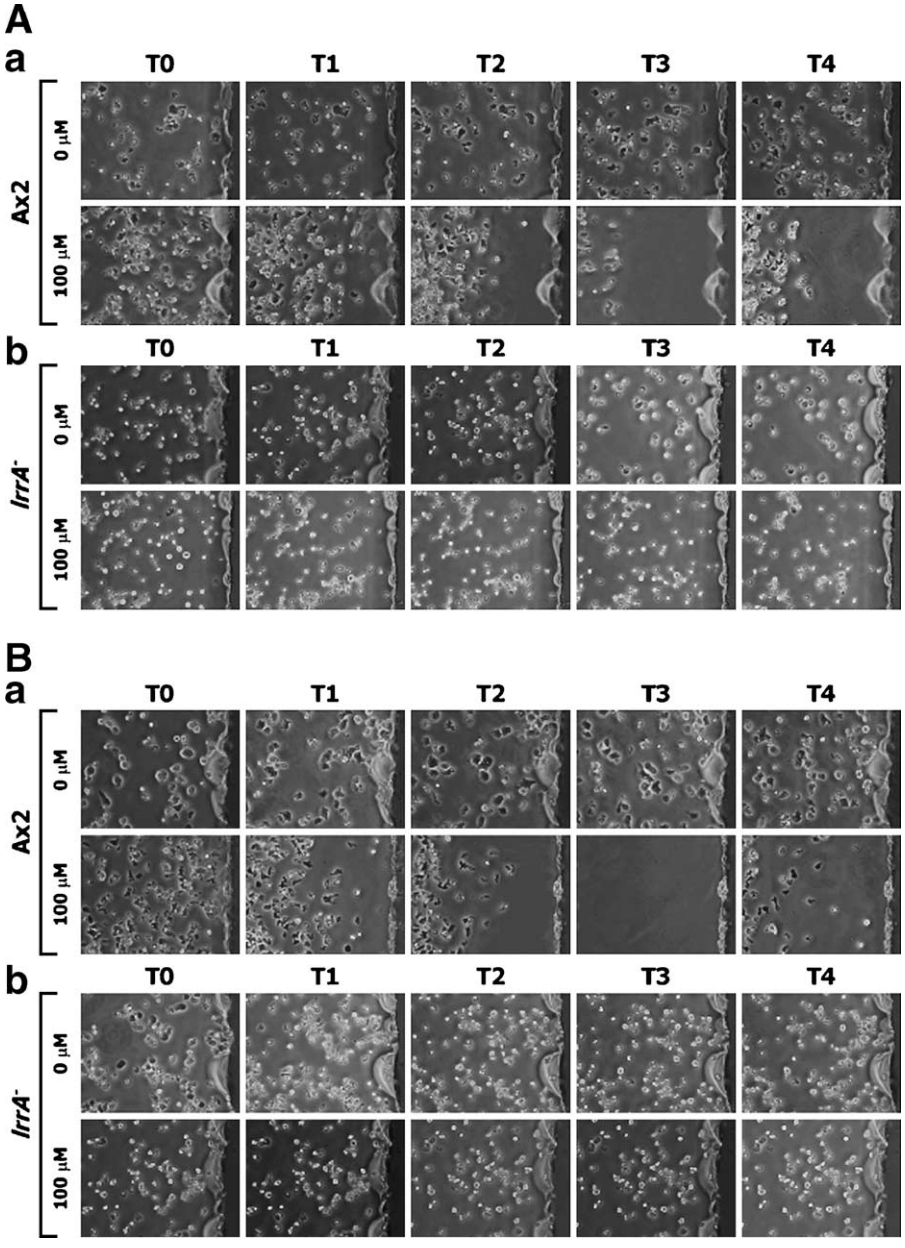

Fig. 6. Dunn chamber chemotaxis assay of the *lrrA*$^-$ cells to gradients of folic acid. Vegetative amoebae (A) and starved 6 h cells (B) were plated on cover slips, and then the cover slips with cells were inverted onto the Dunn chamber slide. Developing buffer in outer well contained 100 μM of folic acid as indicated. The photographs were taken every hour after setting up the Dunn chamber. The inner well is toward the right.

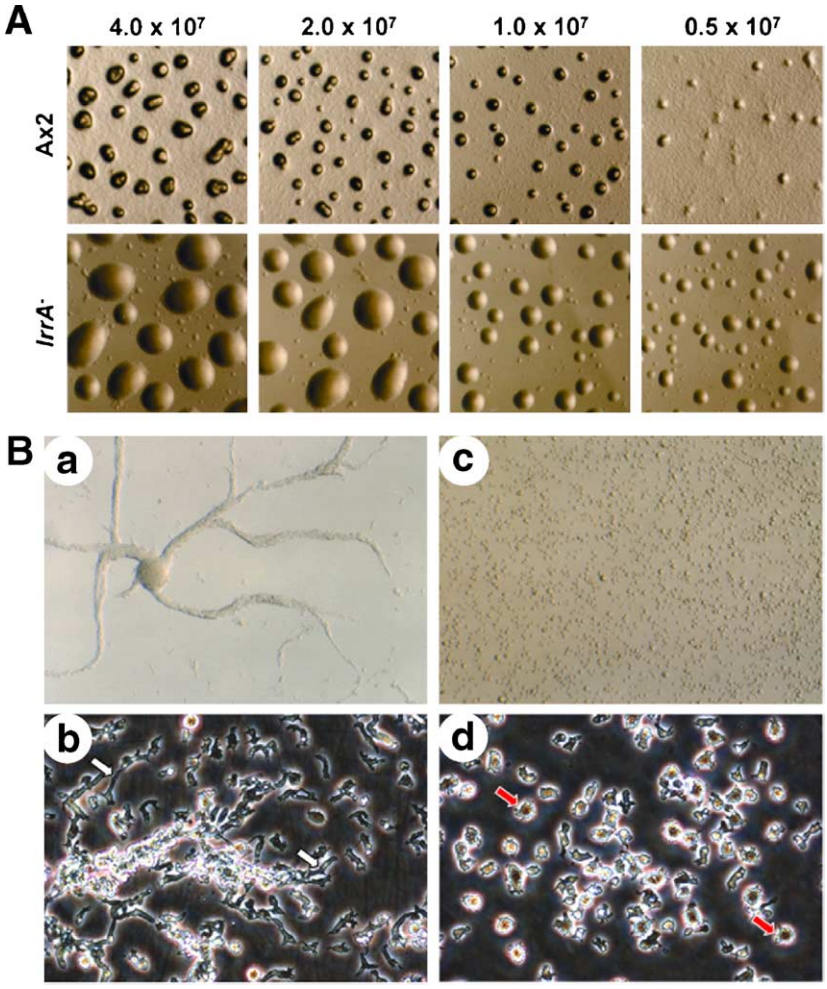

Fig. 7. Aggregation patterns of the *lrrA*$^-$ cells. (A) Aggregation of the *lrrA*$^-$ cells at different cell densities. Aggregation structures formed by wild-type Ax2 and *lrrA*$^-$ cells at the cell number are as indicated. The photographs were taken after 12 h of development. (B) Aggregation of the *lrrA*$^-$ cells in a submerged monolayer. Representative photographs of aggregation patterns that formed after 13 h of incubation are shown: a and b, wild-type cells; c and d, *lrrA*$^-$ cells. White arrows indicate the elongated and polarized wild-type cells, and red arrows indicate the rounded and nonpolar *lrrA*$^-$ cells.

type cells formed streams of migrating cells joined head to tail as they moved in towards the aggregation center, which was emitting pulses of the chemoattractant cAMP (Fig. 7B).

These results suggested that *lrrA*$^-$ cells were impaired in cAMP signaling during early aggregation. To examine this possibility, wild-type and *lrrA*$^-$ cells were pulsed with 30 nM cAMP for 6 h to mimic the normal oscillatory pulses of cAMP that occur during early aggregation and then were plated on non-nutrient agars. Unlike the response seen in wild-type cells, the *lrrA*$^-$ cells formed aggregates but still arrested at the mound stage without the formation of apical tip (data not shown).

Next, we examined the developmental phenotype of Ax2 and *lrrA*$^-$ cells in mixtures with various ratios. The chimeric aggregates were able to form apical tips and mature fruiting bodies, but the size of the fruiting bodies decreased dramatically when half of the cells in the mixtures were mutant cells (Fig. 8A). In contrast, formation of the tipless aggregates increased significantly in the numbers and sizes with respect to the ratios of mutant cells increases, indicating that disruption of the *lrrA* gene results in sorting out of mutant from wild-type cells during aggregation. These results suggested that *lrrA*$^-$ cells either failed to co-aggregate with wild-type cells or, if co-aggregating, were unable to be rescued by wild-type cells.

To examine the ability of *lrrA*$^-$ cells to sort and form specific structures in these chimeric organisms, we tagged mutant cells with the constitutively expressed reporter construct *act15-gfp*. Most of the *gfp*$^+$ mutant cells were found at the periphery of the mound. Few were found inside the mound, and no GFP-expressed cells were observed in the apical tip domain (Fig. 8B), indicating that most of the *lrrA*$^-$ cells were excluded from cell sorting in the mound. During the post-aggregative stage, the mutant cells sorted preferentially to the rear of the slug and lower cup region of spore head and tended to be lost from the rear of standing and migrating slugs (Fig. 8B). We confirmed these results using the *lacZ* reporter tagged *lrrA*$^-$ cells. The spatial pattern of mutant cells in chimeric organisms with wild-type cells was similar to that observed using GFP labeled *lrrA*$^-$ cells (see Supplementary

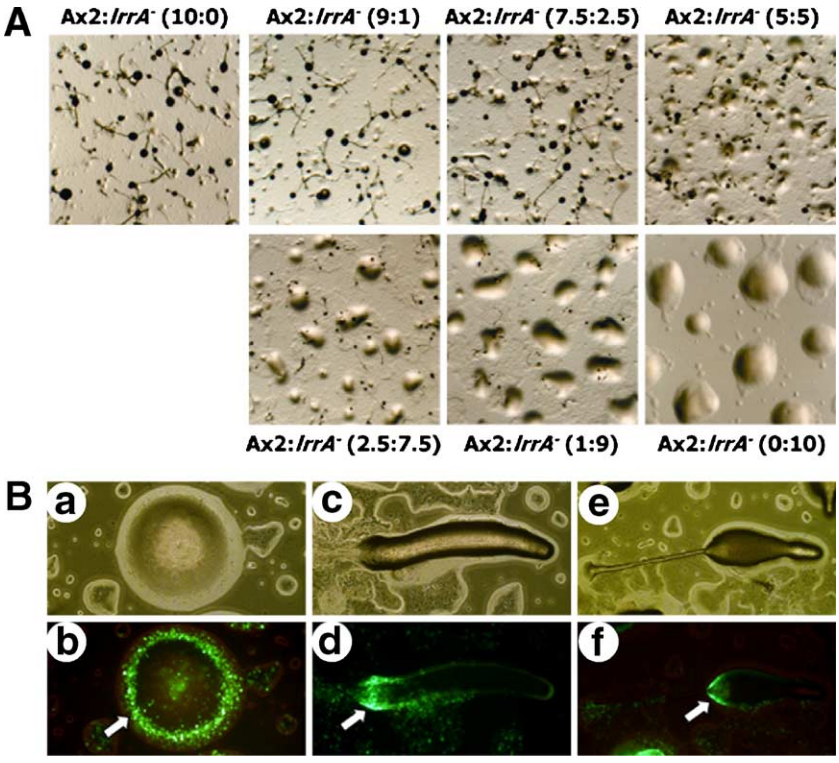

Fig. 8. Developmental morphology and spatial localization of *lrrA*$^-$ cells in chimeric multicellular structures. (A) Developmental morphologies of chimeric multicellular structures of wild-type Ax2 and *lrrA*$^-$ mixed in various ratios as indicated. The samples were photographed after 36 h of development. (B) Fluorescence images of the *lrrA*$^-$ cells expressing *act15-gfp* in chimeric multicellular structures formed in a mixture of 90% wild-type Ax2 and 10% *lrrA*$^-$ at different developmental stages: a and b, mound; c and d, slug; e and f, late culmination stage. White arrows indicate the labeled cells in different chimeric multicellular structures.

data, Supplementary Fig. 3). In addition, when mixed with an excess of wild-type cells, very few of the *lrrA*$^-$ detergent- and heat-resistant spores were formed when spore viability was assayed (<3%; data not shown).

Effects on developmental gene expression

To investigate why *lrrA*$^-$ cells could aggregate to form loose mounds but failed to form streams, we examined the expression of the aggregation-stage genes *aca* (aggregation adenylyl cyclase; Pitt et al., 1992, 1993; Kriebel et al., 2003), *car1* (cAMP receptor 1; Klein et al., 1988; Sun and Devreotes, 1991), *pde* (cAMP phosphodiesterase; Lacombe et al., 1986; Faure et al., 1988, 1990; Hall et al., 1993), *cadA* (calcium-dependent cell adhesion molecule; Wong et al., 1996; Yang et al., 1997) and *csA* (contact site A; Noegel et al., 1986; Desbarats et al., 1992). Northern blots of RNAs extracted from the wild-type and *lrrA*$^-$ cells at various times during development showed that the time of appearance of transcripts of the early genes *aca*, *car1* and *pde* was delayed by roughly 6 h in the mutant and their expression level was markedly reduced (Fig. 9A), indicating that *lrrA*$^-$ cells were impaired in cAMP signaling during early aggregation.

The initial expression of *cadA* was similar in wild-type and mutant cells, but expression thereafter differed, with maximal levels being attained at 9 h in wild-type cells and at 12 h in mutant cells. In wild-type cells, *cadA* expression was down-regulated after 9 h, whereas expression remained elevated in *lrrA*$^-$ cells (Fig. 9A), possibly because of the arrest of the *lrrA*$^-$ cells at the loose mound stage. In *lrrA*$^-$ cells, however, the level of *csA* expression was slightly reduced compared with that of wild-type cells, and the kinetics of induction was delayed by roughly 6 h. In wild-type cells, *csA* expression was down-regulated after 6 h but remained elevated in mutant cells, likely due to the arrest of the mutant cells at the mound stage (Fig. 9A). These results indicated that the defect of streaming in *lrrA*$^-$ cells could not be ascribed to the failure to express cell adhesion molecules, such as DdCAD-1 and csA.

To examine post-aggregative cell-type differentiation, we analyzed the expression of the cell-specific prestalk and prespore genes, *ecmA* and *psA* (Ceccarelli et al., 1987; Jermyn et al., 1987; Early et al., 1988a,b). In *lrrA*$^-$ cells, *ecmA* and *psA* expression was delayed by roughly 4 h, and their level of expression was greatly decreased (Fig. 9B), again pointing to very limited post-aggregative development.

Discussion

In this study, we identified and analyzed the biological function of novel protein, LrrA, in *D. discoideum*. LrrA

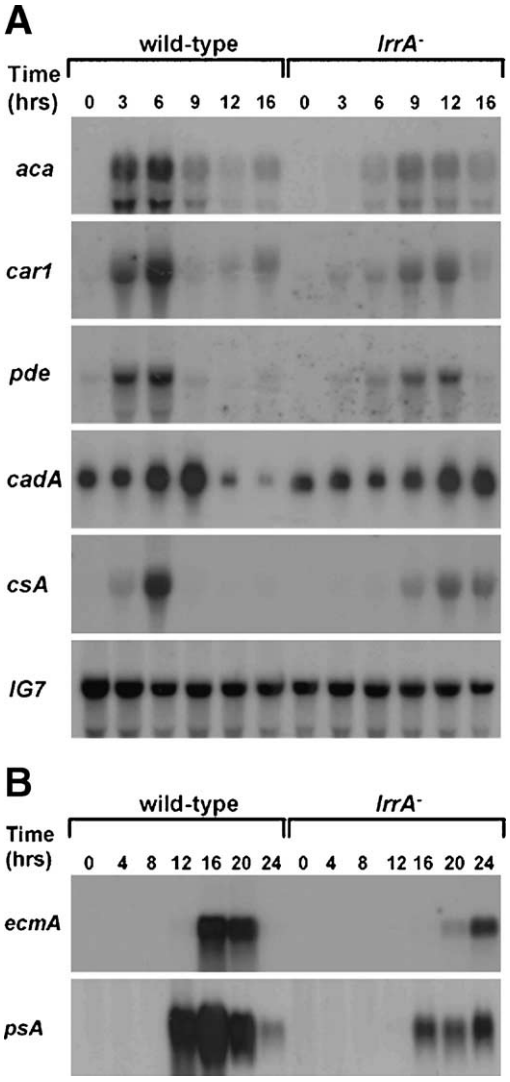

Fig. 9. Effect of the *lrrA* null mutation on developmental gene expression. Northern blot analysis of total RNA isolated from wild-type Ax2 and *lrrA*$^-$ cells at various times of development as indicated. (A) Expression of developmentally regulated genes during early aggregation: *aca* (aggregation adenylyl cyclase), *car1* (cAMP receptor 1), *pde* (cAMP phosphodiesterase), *cadA* (calcium-dependent cell adhesion molecule) and *csA* (contact site A). *IG7* is expressed at a constant level during development and is used as a reference. (B) Expression of cell-type-specific genes during post-aggregative stage: *psA* (prespore-specific cell surface glycoprotein) and *ecmA* (prestalk-specific extracellular matrix protein).

consists almost entirely of a series of nineteen 23-amino-acid LRRs that constitute more than 85% of the total amino acid sequence of the protein. No other functional modules apart from a single putative leucine zipper motif are present. The consensus residues, PxxIGxLxxLxxLxLxxNxLxxL, in all 19 repeats strongly resemble the LRRs in the proteins Cyr1p and SUR-8, which mediate interactions of both proteins with Ras proteins (Field et al., 1990; Suzuki et al., 1990; Sieburth et al., 1998; Li et al., 2000). The existence of such repeats and of additional consensus residues in particular proline suggests that the LrrA protein may function in a manner analogous to a Ras interacting protein.

D. discoideum expresses a large number of Ras proteins with a wide range of functions during vegetative growth and development (Chubb and Insall, 2001; Wilkins and Insall, 2001; Lim et al., 2002). For instance, the small GTPase RasG protein may control the actin cytoskeleton and play a role in adhesion (Tuxworth et al., 1997). Cells expressing constitutively active RasG[G12T] show increased cell–substrate adhesion (Chen and Katz, 2000). In addition, the developmental expression of constitutively active RasD [G12T] or RasG[G12T] results in multi-tipped aggregates, which do not undergo further morphogenesis (Reymond et al., 1986; Jaffer et al., 2001). Furthermore, recent studies have identified a novel RasG-interacting protein (RIP3) whose function is required for both chemotaxis and cAMP signaling (Lee et al., 1999). In view of the well-established relation between LRRs and Ras proteins, we tested whether LrrA can function as a scaffold protein in Ras signaling pathways. Using the yeast two-hybrid system, we examined the possible interaction between LrrA and RasD[G12T] or RasG[G12T]. We found no indications of such an interaction (S.-Z. Chen, unpublished). While this suggests that LrrA functions independently of interaction with Ras proteins, we cannot exclude the possibility that it interacts with some other Ras protein.

As a novel protein, LrrA clearly plays a decisive role in multicellular morphogenesis, especially in the formation of apical tip. The defect in tip formation in the *lrrA*$^-$ cells is significant as this structure serves as the signaling center in the mound and is essential for differentiation and morphogenesis to proceed. Tip formation is a process of differential cell movement in which prestalk cells sort and accumulate to form the anterior domain of the multicellular structure (Durston and Vork, 1979; Williams et al., 1989; Jermyn et al., 1996; Vasiev and Weijer, 1999). How the tip is formed is still a mystery. Only a handful of genes are defective in tip formation, such as null mutations in *cAR2* (Saxe et al., 1993), *limB* (Chien et al., 2000), *myosin II* (De Lozanne and Spudich, 1987; Knecht and Loomis, 1987; Clow et al., 2000) and *dtfA* (Ginger et al., 1998). The *lrrA*$^-$ mutant defect is similar to that of *limB* null mutant in that they both appear to extend excess actin-rich microspikes and are defective in aggregation (Chien et al., 2000). However, there are differences in the mound morphology and the timing of aggregation; the *limB*$^-$ mounds are of a normal size, but there is a delay in their formation. Thus, LrrA has a distinct role in mound and tip formation.

Formation of a multicellular structure in *D. discoideum* requires cell–cell adhesion. During early development, there are EDTA-sensitive and EDTA-resistant cell–cell adhesions. The former is mediated by DdCAD-1 (Brar and Siu, 1993; Wong et al., 1996) and the latter by csA (Siu et al., 1985). The earliest detectable phenotypic trait in *lrrA*$^-$ cells is a defect in cell-substratum adhesion. Presently, cell adhesion analyses revealed that *lrrA*$^-$ cells are adhesion defective. Northern blot analysis of cell adhesion molecules showed that the expression level of *cadA* and *csA* in *lrrA*$^-$

cells is roughly similar to that of the wild-type, but the expression kinetics of both genes is markedly delayed. These results indicate that *lrrA*$^-$ cells are capable of aggregating to form larger loose mounds but are incapable of aggregating tightly to form an apical tip to organize the subsequent morphogenesis rather than to the inability to express cell adhesion molecules such as DdCAD-1 and csA. In addition, microscopic examination of single aggregation stage cells demonstrated that *lrrA*$^-$ cells do not become polarized and have defects in actin organization by extending more F-actin enriched microspikes. This abnormal cell shape may reduce the ability to make physical contacts and again contribute to its developmental phenotype. These results indicate that LrrA plays an important role in both adhesion and cytoskeleton remodeling during early development in *D. discoideum*.

In conclusion, our results clearly indicate that LrrA is not needed for cell growth but is required for effective adhesion to the substratum and to other cells, which is absolutely essential for the formation of apical tip and subsequent developmental morphogenesis. This is entirely consistent with the primary function of the LRR motifs to provide a versatile structural framework for the protein–protein interactions (Kajava, 1998; Kobe and Kajava, 2001). Our preliminary analyses from a comparative protein structural modeling analysis (SWISS-MODEL, the GlaxoSmithKline, Geneva, Switzerland; http://www.expasy.ch/swissmod/SWISS-MODEL.html) and a fully automated protein structure meta prediction system (3D-Jury, http://BioInfo.PL/Meta; Ginalski et al., 2003; Ginalski and Rychlewski, 2003) indicate that the LRR motif in the LrrA protein resembles the structure of LRRs in *Listeria monocytogenes* internalin (InlA), which mediates bacterial adhesion and invasion of epithelial cells in the human intestine through specific interaction with its host cell receptor E-cadherin (Schubert et al., 2001, 2002), suggesting that LrrA might function as a scaffold in protein–protein interaction (T.-L. Cheng, unpublished). To elucidate the biochemical function of the LrrA protein in the cytoskeleton remodeling during multicellular morphogenesis, it will be useful to identify protein(s) that interact with it.

Acknowledgments

We thank the *Dictyostelium* cDNA project in Japan for kindly providing the original cDNA clone FCL-AC05. This work was supported by grants from the National Science Council of Taiwan, ROC (to Wen-Tsan Chang).

Appendix A. Supplementary data

Supplementary data associated with this article can be found, in the online version, at doi:10.1016/j.ydbio.2005.05.045.

References

Allen, W.E., Zicha, D., Ridley, A.J., Jones, G.E., 1998. A role for Cdc42 in macrophage chemotaxis. J. Cell Biol. 141, 1147–1157.

Aubry, L., Firtel, R.A., 1999. Integration of signaling networks that regulate *Dictyostelium* differentiation. Annu. Rev. Cell Dev. Biol. 15, 469–517.

Ausubel, F.M., Brent, R., Kingston, R.E., Moore, D.D., Seidman, J.G., Smith, J.A., Struhl, K., 1998. Current Protocols in Molecular Biology. John Wiley and Sons, New York.

Bilder, D., Perrimon, N., 2000. Localization of apical epithelial determinants by the basolateral PDZ protein Scribble. Nature 403, 676–680.

Brar, S.K., Siu, C.H., 1993. Characterization of the cell adhesion molecule gp24 in *Dictyostelium discoideum*. Mediation of cell–cell adhesion via a Ca^{2+}-dependent mechanism. J. Biol. Chem. 268, 24902–24909.

Buchanan, S.G.ST.C., Gay, N.J., 1996. Structural and functional diversity in the leucine-rich repeat family of proteins. Prog. Biophys. Mol. Biol. 65, 1–44.

Ceccarelli, A., McRobbie, S.J., Jermyn, K.A., Duffy, K., Early, A., Williams, J.G., 1987. Structural and functional characterization of a *Dictyostelium* gene encoding a DIF inducible, prestalk-enriched mRNA sequence. Nucleic Acids Res. 15, 7463–7476.

Chang, W.-T., Gross, J.D., Newell, P.C., 1995. Trapping developmental promoters in *Dictyostelium*. Plasmid 34, 175–183.

Chang, W.-T., Newell, P.C., Gross, J.D., 1996. Identification of the cell fate gene *stalky* in *Dictyostelium*. Cell 87, 471–481.

Chen, C.F., Katz, E.R., 2000. Mediation of cell-substratum adhesion by RasG in *Dictyostelium*. J. Cell. Biochem. 79, 139–149.

Chen, M.Y., Insall, R.H., Devreotes, P.N., 1996. Signaling through chemoattractant receptors in *Dictyostelium*. Trends Genet. 12, 52–57.

Chien, S., Chung, C.Y., Sukumaran, S., Osborne, N., Lee, S., Ellsworth, C., McNally, J.G., Firtel, R.A., 2000. The *Dictyostelium* LIM domain-containing protein LIM2 is essential for proper chemotaxis and morphogenesis. Mol. Biol. Cell 11, 1275–1291.

Chubb, J.R., Insall, R.H., 2001. *Dictyostelium*: an ideal organism for genetic dissection of Ras signalling networks. Biochim. Biophys. Acta 1525, 262–271.

Clow, P.A., McNally, J.G., 1999. In vivo observations of myosin II dynamics support a role in rear retraction. Mol. Biol. Cell 10, 1309–1323.

Clow, P.A., Chen, T., Chisholm, R.L., McNally, J.G., 2000. Three-dimensional in vivo analysis of *Dictyostelium* mounds reveals directional sorting of prestalk cells and defines a role for the myosin II regulatory light chain in prestalk cell sorting and tip protrusion. Development 127, 2715–2728.

Crameri, A., Whitehorn, E., Tate, E., Stemmer, W.P.C., 1996. Improved green fluorescent protein by molecular evolution using DNA shuffling. Nat. Biotechnol. 14, 315–319.

De Lozanne, A., 1987. Homologous recombination in *Dictyostelium* as a tool for the study of developmental genes. Methods Cell Biol. 28, 489–495.

De Lozanne, A., Spudich, J.A., 1987. Disruption of the *Dictyostelium* myosin heavy chain gene by homologous recombination. Science 236, 1086–1091.

Desbarats, L., Lam, T.Y., Wong, L.M., Siu, C.H., 1992. Identification of a unique cAMP-response element in the gene encoding the cell adhesion molecule gp80 in *Dictyostelium discoideum*. J. Biol. Chem. 267, 19655–19664.

Devreotes, P.N., 1989. *Dictyostelium discoideum*: a model system for cell–cell interactions in development. Science 245, 1054–1058.

Dormann, D., Vasiev, B., Weijer, C.J., 2000. The control of chemotactic cell movement during *Dictyostelium* morphogenesis. Philos. Trans. R. Soc. Lond., Ser. B Biol. Sci. 355, 983–991.

Durston, A.J., Vork, F., 1979. A cinematographical study of the development of vitally stained *Dictyostelium discoideum*. J. Cell Sci. 36, 261–279.

Dynes, J.L., Clark, A.M., Shaulsky, G., Kuspa, A., Loomis, W.F., Firtel, R.A., 1994. LagC is required for cell–cell interactions that are essential for cell-type differentiation in *Dictyostelium*. Genes Dev. 8, 948–958.

Early, A.E., McRobbie, S.J., Duffy, K.T., Jermyn, K.A., Tilly, R., Ceccarelli, A., Williams, J.G., 1988a. Structural and functional characterization of genes encoding *Dictyostelium* prestalk and prespore cell-specific proteins. Dev. Genet. 9, 383–402.

Early, A.E., Williams, J.G., Meyer, H.E., Por, S.B., Smith, E., Williams, K.L., Gooley, A.A., 1988b. Structural characterization of *Dictyostelium discoideum* prespore-specific gene D19 and of its product, cell surface glycoprotein PsA. Mol. Cell. Biol. 8, 3458–3466.

Early, A.E., Abe, T., Williams, J.G., 1995. Evidence for positional differentiation of prestalk cells and for a morphogenetic gradient in *Dictyostelium*. Cell 83, 91–99.

Faure, M., Podgorski, G.J., Franke, J., Kessin, R.H., 1988. Disruption of *Dictyostelium discoideum* morphogenesis by overproduction of cAMP phosphodiesterase. Proc. Natl. Acad. Sci. U. S. A. 85, 8076–8080.

Faure, M., Franke, J., Hall, A.L., Podgorski, G.J., Kessin, R.H., 1990. The cyclic nucleotide phosphodiesterase gene of *Dictyostelium discoideum* contains three promoters specific for growth, aggregation, and late development. Mol. Cell. Biol. 10, 1921–1930.

Field, J., Xu, H.-P., Michaeli, T., Ballester, R., Sass, P., Wigler, M., Colicelli, J., 1990. Mutations of the adenylyl cyclase gene that block RAS function in *Saccharomyces cerevisiae*. Science 247, 464–467.

Firtel, R.A., 1995. Integration of signaling information in controlling cell-fate decisions in *Dictyostelium*. Genes Dev. 9, 1427–1444.

Firtel, R.A., 1996. Interacting signaling pathways controlling multicellular development in *Dictyostelium*. Curr. Opin. Genet. Dev. 6, 545–554.

Firtel, R.A., Meili, R., 2000. *Dictyostelium*: a model for regulated cell movement during morphogenesis. Curr. Opin. Genet. Dev. 10, 421–427.

Ginalski, K., Rychlewski, L., 2003. Detection of reliable and unexpected protein fold predictions using 3D-Jury. Nucleic Acids Res. 31, 3291–3292.

Ginalski, K., Elofsson, A., Fischer, D., Rychlewski, L., 2003. 3D-Jury: a simple approach to improve protein structure predictions. Bioinformatics 19, 1015–1018.

Ginger, R.S., Drury, L., Baader, C., Zhukovskaya, N.V., Williams, J.G., 1998. A novel *Dictyostelium* cell surface protein important for both cell adhesion and cell sorting. Development 125, 3343–3352.

Gross, J.D., 1994. Developmental decisions in *Dictyostelium discoideum*. Microbiol. Rev. 58, 330–351.

Hall, A.L., Franke, J., Faure, M., Kessin, R.H., 1993. The role of the cyclic nucleotide phosphodiesterase of *Dictyostelium discoideum* during growth, aggregation, and morphogenesis: overexpression and localization studies with the separate promoters of the pde. Dev. Biol. 157, 73–84.

Huang, Y.-C., Chen, Y.-H., Lo, S.-R., Liu, C.-I., Wang, C.-W., Chang, W.-T., 2004. Disruption of the peroxisomal citrate synthase CshA affects cell growth and multicellular development in *Dictyostelium discoideum*. Mol. Microbiol. 53, 81–91.

Inohara, N., Nunez, G., 2001. The NOD: a signaling module that regulates apoptosis and host defense against pathogens. Oncogene 20, 6473–6481.

Inohara, N., Koseki, T., del Peso, L., Hu, Y., Yee, C., Chen, S., Carrio, R., Merino, J., Liu, D., Ni, J., Nunez, G., 1999. Nod1, an Apaf-1-like activator of caspase-9 and nuclear factor-kappaB. J. Biol. Chem. 274, 14560–14567.

Jaffer, Z.M., Khosla, M., Spiegelman, G.B., Weeks, G., 2001. Expression of activated Ras during *Dictyostelium* development alters cell localization and changes cell fate. Development 128, 907–916.

Jermyn, K.A., Berks, M., Kay, R.R., Williams, J.G., 1987. Two distinct classes of prestalk-enriched mRNA sequences in *Dictyostelium discoideum*. Development 100, 745–755.

Jermyn, K., Traynor, D., Williams, J., 1996. The initiation of basal disc formation in *Dictyostelium discoideum* is an early event in culmination. Development 122, 753–760.

Kajava, A.V., 1998. Structural diversity of leucine-rich repeat proteins. J. Mol. Biol. 277, 519–527.

Kataoka, T., Broek, D., Wigler, M., 1985. DNA sequence and characterization of the *S. cerevisiae* gene encoding adenylate cyclase. Cell 43, 493–505.

Kellerman, K.A., McNally, J.G., 1999. Mound-cell movement and morphogenesis in *Dictyostelium*. Dev. Biol. 208, 416–429.

Kibler, K., Svetz, J., Nguyen, T.L., Shaw, C., Shaulsky, G., 2003. A cell-adhesion pathway regulates intercellular communication during *Dictyostelium* development. Dev. Biol. 264, 506–521.

Klein, P.S., Sun, T.J., Saxe III, C.L., Kimmel, A.R., Johnson, R.L., Devreotes, P.N., 1988. A chemoattractant receptor controls development in *Dictyostelium discoideum*. Science 241, 1467–1472.

Knecht, D.A., Loomis, W.F., 1987. Antisense RNA inactivation of myosin heavy chain gene expression in *Dictyostelium discoideum*. Science 236, 1081–1086.

Kobe, B., Deisenhofer, J., 1994. The leucine-rich repeat: a versatile binding motif. Trends Biochem. Sci. 19, 415–421.

Kobe, B., Deisenhofer, J., 1995. Proteins with leucine-rich repeats. Curr. Opin. Struct. Biol. 5, 409–416.

Kobe, B., Kajava, A.V., 2001. The leucine-rich repeat as a protein recognition motif. Curr. Opin. Struct. Biol. 11, 725–732.

Kriebel, P.W., Barr, V.A., Parent, C.A., 2003. Adenylyl cyclase localization regulates streaming during chemotaxis. Cell 112, 549–560.

Lacombe, M.L., Podgorski, G.J., Franke, J., Kessin, R.H., 1986. Molecular cloning and developmental expression of the cyclic nucleotide phosphodiesterase gene of *Dictyostelium discoideum*. J. Biol. Chem. 261, 16811–16817.

Lee, S., Parent, C.A., Insall, R., Firtel, R.A., 1999. A novel Ras-interacting protein required for chemotaxis and cyclic adenosine monophosphate signal relay in *Dictyostelium*. Mol. Biol. Cell 10, 2829–2845.

Li, W., Han, M., Guan, K.-L., 2000. The leucine-rich repeat protein SUR-8 enhances MAP kinase activation and forms a complex with Ras and Raf. Genes Dev. 14, 895–900.

Lim, C.J., Spiegelman, G.B., Weeks, G., 2002. Cytoskeletal regulation by *Dictyostelium* Ras subfamily proteins. J. Muscle Res. Cell Motil. 23, 729–736.

Nicol, A., Rappel, W., Levine, H., Loomis, W.F., 1999. Cell-sorting in aggregates of *Dictyostelium discoideum*. J. Cell Sci. 112, 3923–3929.

Noegel, A., Gerisch, G., Stadler, J., Westphal, M., 1986. Complete sequence and transcript regulation of a cell adhesion protein from aggregating *Dictyostelium* cells. EMBO J. 5, 1473–1476.

Pan, P., Hall, E.M., Bonner, J.T., 1972. Folic acid as second chemotactic substance in the cellular slime moulds. Nat., New Biol. 237, 181–182.

Pan, P., Hall, E.M., Bonner, J.T., 1975. Determination of the active portion of the folic acid molecule in cellular slime mold chemotaxis. J. Bacteriol. 122, 185–191.

Parent, C.A., Devreotes, P.N., 1996. Molecular genetics of signal transduction in *Dictyostelium*. Annu. Rev. Biochem. 65, 411–440.

Pitt, G.S., Milona, N., Borleis, J., Lin, K.C., Reed, R.R., Devreotes, P.N., 1992. Structurally distinct and stage-specific adenylyl cyclase genes play different roles in *Dictyostelium* development. Cell 69, 305–315.

Pitt, G.S., Brandt, R., Lin, K.C., Devreotes, P.N., Schaap, P., 1993. Extracellular cAMP is sufficient to restore developmental gene expression and morphogenesis in *Dictyostelium* cells lacking the aggregation adenylyl cyclase (ACA). Genes Dev. 7, 2172–2180.

Reymond, C.D., Gomer, R.H., Nellen, W., Theibert, A., Devreotes, P., Firtel, R.A., 1986. Phenotypic changes induced by a mutated ras gene during the development of *Dictyostelium* transformants. Nature 323, 340–343.

Reymond, C.D., Schaap, P., Veron, M., Williams, J.G., 1995. Dual role of cAMP during *Dictyostelium* development. Experientia 51, 1166–1174.

Rubin, J., Robertson, A., 1975. The tip of the *Dictyostelium discoideum* pseudoplasmodium as an organizer. J. Embryol. Exp. Morphol. 33, 227–241.

Sambrook, J., Fritsch, E.F., Maniatis, T., 1989. Molecular Cloning: A Laboratory Manual, 2nd ed. Cold Spring Harbor Laboratory Press, Cold Spring Harbor, NY.

Saxe III, C.L., Ginsburg, G.T., Louis, J.M., Johnson, R., Devreotes, P.N., Kimmel, A.R., 1993. CAR2, a prestalk cAMP receptor required for

normal tip formation and late development of *Dictyostelium discoideum*. Genes Dev. 7, 262–272.

Schubert, W.D., Gobel, G., Diepholz, M., Darji, A., Kloer, D., Hain, T., Chakraborty, T., Wehland, J., Domann, E., Heinz, D.W., 2001. Internalins from the human pathogen *Listeria monocytogenes* combine three distinct folds into a contiguous internalin domain. J. Mol. Biol. 312, 783–794.

Schubert, W.D., Urbanke, C., Ziehm, T., Beier, V., Machner, M.P., Domann, E., Wehland, J., Chakraborty, T., Heinz, D.W., 2002. Structure of internalin, a major invasion protein of *Listeria monocytogenes*, in complex with its human receptor E-cadherin. Cell 111, 825–836.

Shaulsky, G., Loomis, W.F., 1996. Initial cell type divergence in *Dictyostelium* is independent of DIF-1. Dev. Biol. 174, 214–220.

Sieburth, D.S., Sun, Q., Han, M., 1998. SUR-8, a conserved Ras-binding protein with leucine-rich repeats, positively regulates Ras-mediated signaling in *C. elegans*. Cell 94, 119–130.

Siu, C.H., Lam, T.Y., Choi, A.H., 1985. Inhibition of cell–cell binding at the aggregation stage of *Dictyostelium discoideum* development by monoclonal antibodies directed against an 80,000-dalton surface glycoprotein. J. Biol. Chem. 260, 16030–16036.

Stege, J.T., Shaulsky, G., Loomis, W.F., 1997. Sorting of the initial cell types in *Dictyostelium* is dependent on the tipA gene. Dev. Biol. 185, 34–41.

Sun, T.J., Devreotes, P.N., 1991. Gene targeting of the aggregation stage cAMP receptor cAR1 in *Dictyostelium*. Genes Dev. 5, 572–582.

Suzuki, N., Choe, H.-R., Nishida, Y., Yamawaki-Kataoka, Y., Ohnishi, S., Tamaoki, T., Kataoka, T., 1990. Leucine-rich repeats and carboxyl terminus are required for interaction of yeast adenylate cyclase with RAS proteins. Proc. Natl. Acad. Sci. U. S. A. 87, 8711–8715.

Tong, Z.B., Gold, L., Pfeifer, K.E., Dorward, H., Lee, E., Bondy, C.A., Dean, J., Nelson, L.M., 2000a. Mater, a maternal effect gene required for early embryonic development in mice. Nat. Genet. 26, 267–268.

Tong, Z.B., Nelson, L.M., Dean, J., 2000b. Mater encodes a maternal protein in mice with a leucine-rich repeat domain homologous to porcine ribonuclease inhibitor. Mamm. Genome 11, 281–287.

Traynor, D., Kessin, R.H., Williams, J.G., 1992. Chemotactic sorting to cAMP in the multicellular stages of *Dictyostelium* development. Proc. Natl. Acad. Sci. U. S. A. 89, 8303–8307.

Traynor, D., Tasaka, M., Takeuchi, I., Williams, J.G., 1994. Aberrant pattern formation in myosin heavy chain mutants of *Dictyostelium*. Development 120, 591–601.

Tuxworth, R.I., Cheetham, J.L., Machesky, L.M., Spiegelmann, G.B., Weeks, G., Insall, R.H., 1997. *Dictyostelium* RasG is required for normal motility and cytokinesis, but not growth. J. Cell Biol. 138, 605–614.

Varney, T.R., Casademunt, E., Ho, H.N., Petty, C., Dolman, J., Blumberg, D.D., 2002. A novel *Dictyostelium* gene encoding multiple repeats of adhesion inhibitor-like domains has effects on cell–cell and cell–substrate adhesion. Dev. Biol. 243, 226–248.

Vasiev, B., Weijer, C.J., 1999. Modeling chemotactic cell sorting during *Dictyostelium discoideum* mound formation. Biophys. J. 76, 595–605.

Verkerke-van Wijk, I., Fukuzawa, M., Devreotes, P.N., Schaap, P., 2001. Adenylyl cyclase A expression is tip-specific in *Dictyostelium* slugs and directs StatA nuclear translocation and CudA gene expression. Dev. Biol. 234, 151–160.

Vogel, G., 1987. Endocytosis and recognition mechanisms in *Dictyostelium discoideum*. Methods Cell Biol. 28, 129–137.

Wang, J., Hou, L., Awrey, D., Loomis, W.F., Firtel, R.A., Siu, C.H., 2000. The membrane glycoprotein gp150 is encoded by the lagC gene and mediates cell–cell adhesion by heterophilic binding during *Dictyostelium* development. Dev. Biol. 227, 734–745.

Webb, S.E., Pollard, J.W., Jones, R.E., 1996. Direct observation and quantification of macrophage chemoattraction to the growth factor CSF-1. J. Cell Sci. 109, 793–803.

Wilkins, A., Insall, R.H., 2001. Small GTPase in *Dictyostelium*: lessons from a social amoeba. Trends Genet. 17, 41–48.

Williams, J.G., Duffy, K.T., Lane, D.P., McRobbie, S.J., Harwood, A.J., Traynor, D., Kay, R.R., Jermyn, K.A., 1989. Origins of the prestalk-prespore pattern in *Dictyostelium* development. Cell 59, 1157–1163.

Witke, W., Schleicher, M., Noegel, A.A., 1992. Redundancy in the microfilament system: abnormal development of *Dictyostelium* cells lacking two F-actin cross-linking proteins. Cell 68, 53–62.

Wong, E.F., Brar, S.K., Sesaki, H., Yang, C., Siu, C.H., 1996. Molecular cloning and characterization of DdCAD-1, a Ca^{2+}-dependent cell–cell adhesion molecule, in *Dictyostelium discoideum*. J. Biol. Chem. 271, 16399–16408.

Wu, H., Maciejewski, M.W., Marintchev, A., Benashski, S.E., Mullen, G.P., King, S.M., 2000. Solution structure of a dynein motor domain associated light chain. Nat. Struct. Biol. 7, 575–579.

Xu, P., Mitchelhill, K.I., Kobe, B., Kemp, B.E., Zot, H.G., 1997. The myosin-I-binding protein Acan125 binds the SH3 domain and belongs to the superfamily of leucine-rich repeat proteins. Proc. Natl. Acad. Sci. U. S. A. 94, 3685–3690.

Yang, C., Brar, S.K., Desbarats, L., Siu, C.H., 1997. Synthesis of the Ca^{2+}-dependent cell adhesion molecule DdCAD-1 is regulated by multiple factors during *Dictyostelium* development. Differentiation 61, 275–284.

Zicha, D., Dunn, G., Brown, A.F., 1991. A new direct-viewing chemotaxis chamber. J. Cell Sci. 99, 769–775.